The three-dimensional geometry was created, and the computational domain is meshed with unstructured hexahedral grid in the shell as shown in Figure 2.

The geometry studied includes a fluid domain and a solid domain. For discretization, an unstructured mesh is generated in hexahedral elements adopted in the shell. Several tests were carried out (Table 3) in order to ensure the independence of the results with respect to the mesh adopted namely 491588 cells, 602587 cells and 805874 cells for the profile of the speed and the temperature in the section y = 0.045m.

Table 3. Validation of the mesh at the outlet of the shell

Grid	U_{max}	V_{max}	W_{max}	T_{max}
491588	0,00009	2,0404	0,0027	325,4014
602587	0,0001	2,0573	0,003	325,5871
805874	0,00011	2,0552	0,0029	325,2587

The results presented above show that the variation is very small and does not exceed 1%. The analysis of the results presented show that the choice of (805874) elements, give a good prediction for the present numerical model.

3.3 Model validation

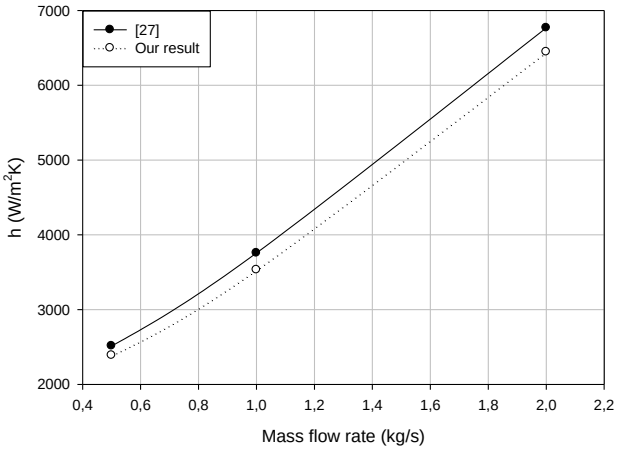

Figure 3. Average heat transfer coefficient

The model with six baffles in Figure 3 is validated with the data are proposed by Ozden and Tari [27], it is found that the overall transfer coefficient of the fluid corresponds to the results of the literature and the difference between the two cases is about 4%.

4. RESULTS

The results obtained from the elaborate calculation code, presented in the form of contours and curves, illustrate the advantage by using baffles in the shell and tube heat exchangers in order to improve their performance.

4.1 Dynamic behavior

4.1.1 Velocity contours

Figures 4 and 5 show the velocity contours in the shell and tube heat exchanger with and without baffles respectively. The velocity contour is represented by colors ranging from green (low velocity) to red (high velocity). From the numerical results it is noted that the values of the velocity are very low in the neighborhood of the walls, because of the presence of the strong gradients of friction. In the annular passage in the case without baffles, the velocity in the upper part of the shell is high and in the lower part is not used properly. In the annular passage in the case with baffles, the fluid velocity is markedly high, the difference in velocity is due to the difference between the two passage sections on the one hand and the presence of the recirculation zones of the water required by the baffle which results in a sudden increase in the dynamic pressure of the water.

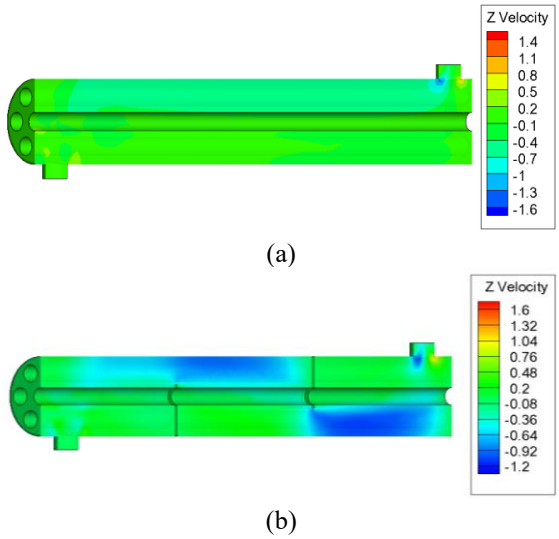

Figure 4. Velocity contours x = 0, (a) without baffles, (b) with baffles

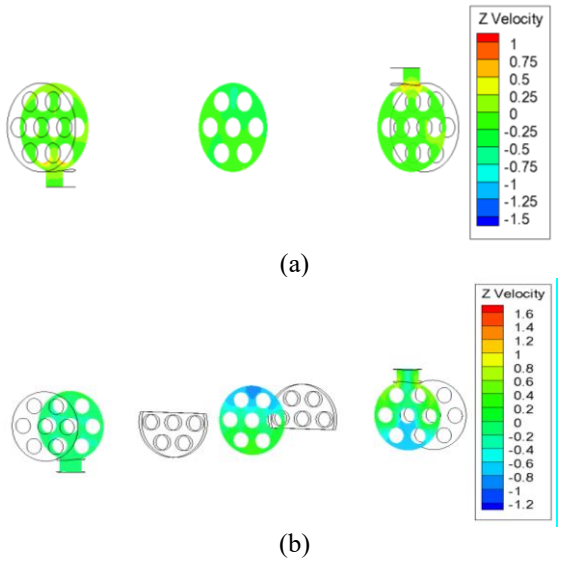

Figure 5. Velocity contours z = 0.58m; z = 0.3m; z = 0.02m, (a) without baffles, (b) with baffles

4.1.2 Velocity profiles in the shell

A presentation of the velocity distribution along the two exchangers in the section y = 0.04m has illustrated in this figure. Figure 6 (a) shows a decrease in the velocity along the shell, the fluid does not encounter any obstacle, its velocity decreases with the sudden enlargement and the lack of baffles.

Figure 6 (b) shows an increase in velocity from the first baffle due to abrupt narrowing of the passage section, is a decrease in velocity from z = 0.02m because the fluid located

in the zone of recirculation after the baffle. The velocity of the flow in the shell of the case without baffle reaches maximum values of the order of 12% of the initial velocity, and in the case with baffles reaches 19% of the initial velocity.

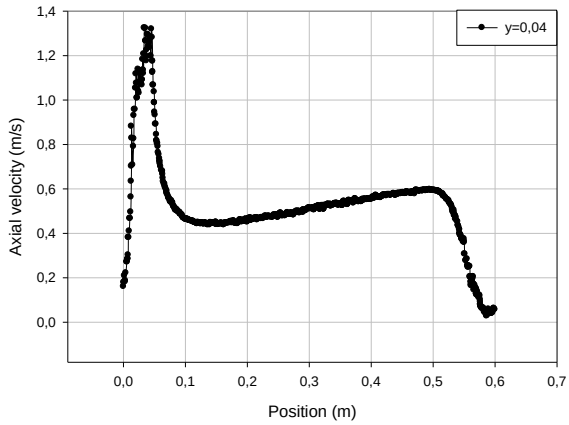

(a)

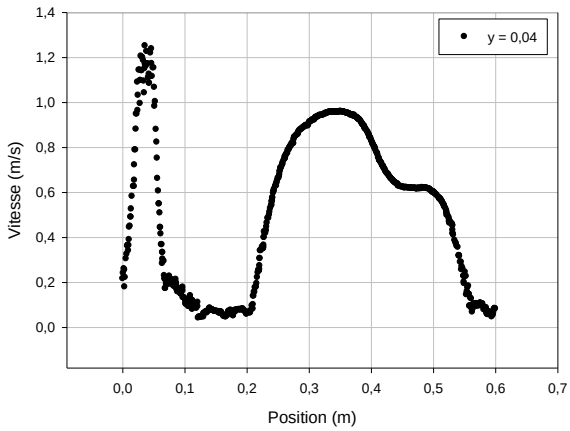

(b)

Figure 6. Velocity distribution at y = 0.04m; (a) without baffles, (b) with baffles

4.1.3 Pressure drop in the shell

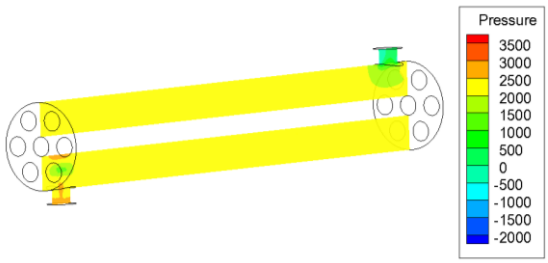

(a)

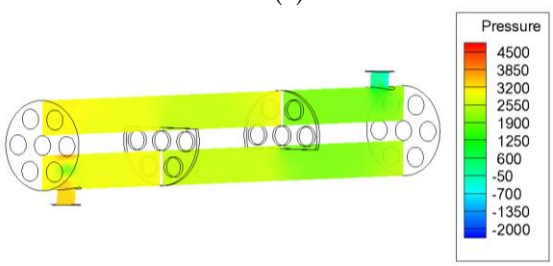

(b)

Figure 7. Pressure drop contours at x = 0, (a) without baffles, (b) with baffles

Figure 7 show the pressure drop in the two shell and tube heat exchangers with baffles and without baffles respectively.

This high pressure drop after the two baffles is caused by, the jet of fluid by high velocity at the baffles breaches, and then the fluid separate of the baffles causes a sudden change in the flow direction and screamed zones of recirculation.

4.2 Thermal behavior

4.2.1 Temperature contours

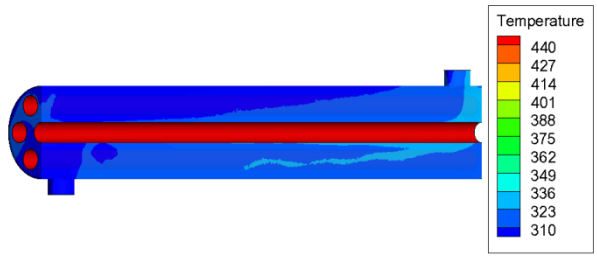

(a)

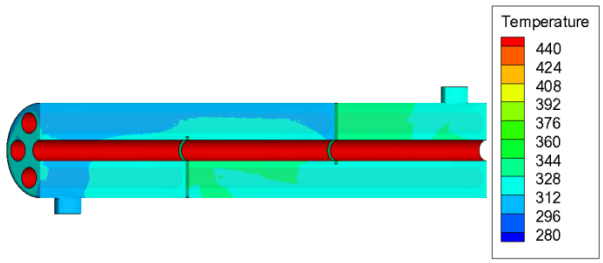

(b)

Figure 8. Temperature contours at x = 0, (a) without baffles, (b) with baffles

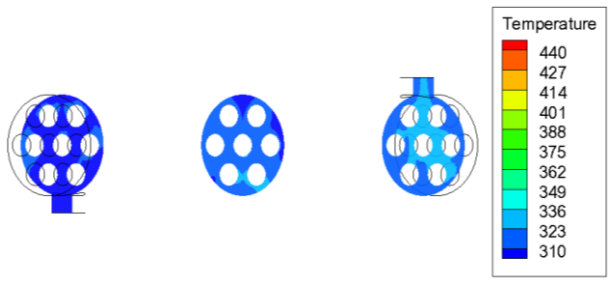

(a)

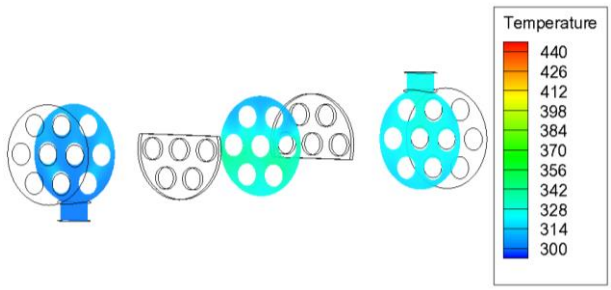

(b)

Figure 9. Temperature contours z = 0.58m; z = 0.3m; z = 0.02m, (a) without baffles, (b) with baffles

Figures 8 and 9 show the isothermal in the two shell and tube heat exchangers with baffles and without baffles respectively. The temperature contour is represented by colors ranging from green (low temperature) to red (high temperature). At the entrance of the two exchangers there is a green outline indicates the temperature of the fluid inlet,

begins to vary from the center of the lower middle of the shell of the case without baffles, varies from the first baffle to the case with baffles. The temperature contours presented for the two cases show an increase in temperature and important values of the region near the tubes and at the level of second baffle. In the case with baffles the field of the temperature shows a low temperature in the first flow passage and an average temperature in the second passage to the baffles.

4.2.2 Temperature profiles in the shell

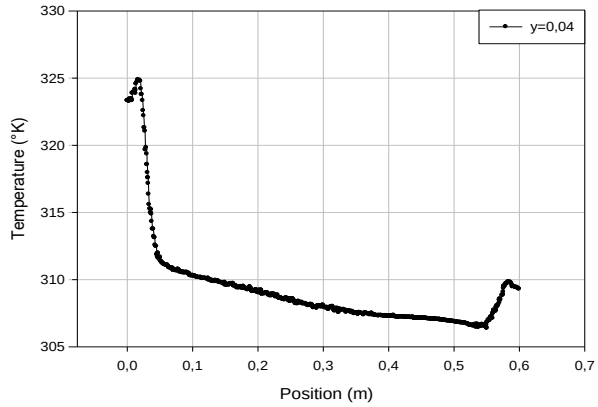

(a)

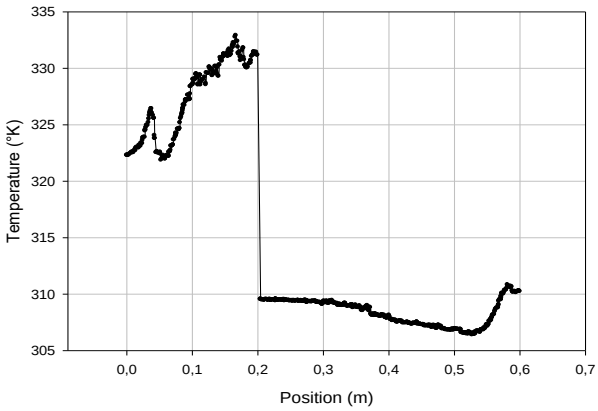

(b)

Figure 10. Temperature distribution at y = 0.04m, (a) without baffles, (b) with baffles

In Figure 10 (a) it is found that the fluid temperature increases slightly in the shell, the lack of baffles, is an additional factor of attenuation of the turbulence in the shell.

In Figure 10 (b) it is found that in the regions after the baffle the temperature is increased sharply. The fluid temperature increases as soon as the fluid is again in contact with the baffle, because the change in the direction of flow produced by the baffle, the highest value of the temperature appears behind the baffle.

4.3 Study of velocity and temperature profiles around 2nd baffle

The understanding of the baffle effect studied can be quantified by plotting the velocity and temperature profiles namely upstream (z = 0.15m) downstream (z = 0.25m) of the baffle for the two configurations.

There is a slight deformation of the velocity field in the two sections in the case without baffles; the decreased of velocity following the axis of the flow is its maximum value of this configuration is 0.52m/s. The impact of the baffles on the structure of the turbulent flow is shown in Figure 11, we clearly see a strong deformation of the velocity field close to the baffle, the velocity profile is tightening more and more in the upper part of the shell before the baffle and in the lower part of the shell after the baffle, while in its free segment, the flow begins to accelerate, the maximum value to observe after the baffle and 1,15m/s.

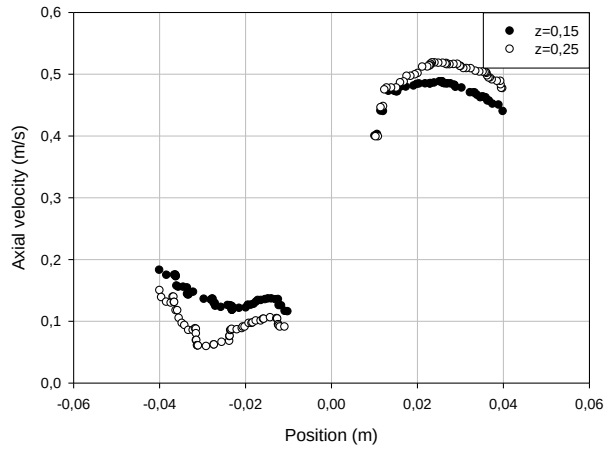

(a)

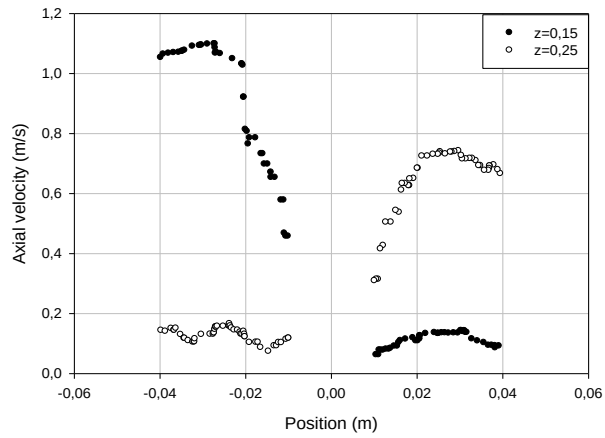

(b)

Figure 11. Velocity profile, (a) without baffles, (b) with baffles

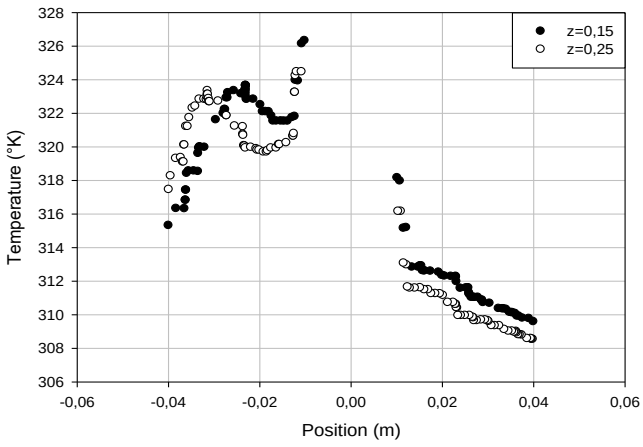

(a)

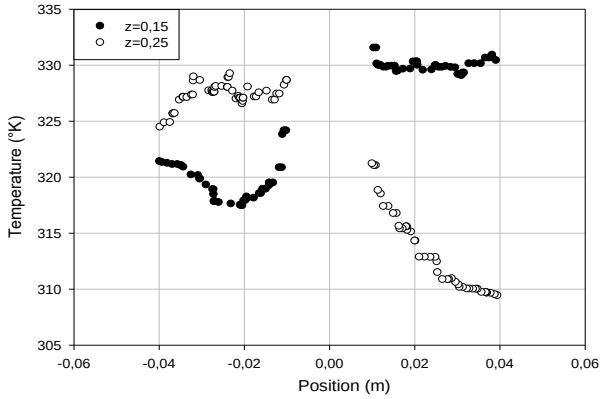

(b)

Figure 12. Temperature profile, (a) without baffles, (b) with baffles

The flow structure in the case with baffles is characterized by large deformations and large recirculation regions; it will significantly influence the distribution of the temperature field and will allow a better mixing of the fluid that will stimulate the heat transfer. If we take the same for y = 0.04m for the two studied cases we have, for the simple case the fluid temperature is 308.5°K and 309.75°K; it is a point having 309°K and 330°K in the case with baffles so clearly clear the role of obstacle in these devices.

4.4 Overall performance factor

Figure 13 shows the performance factor for different mass flow rates. When the mass flow increases the performance decreases because the maximum observed value of the performance index for mass flow 0.5 kg is 12.25 means that the heat transfer coefficient is 12.25 times the greater that the pressure drop, at 2 kg the ratio between these two decisive parameters is 1.58, so the heat transfer coefficient is greater than 1.58 times for the pressure drop. The performance evaluation factor decreased because the contact time to the tubes is decreased.

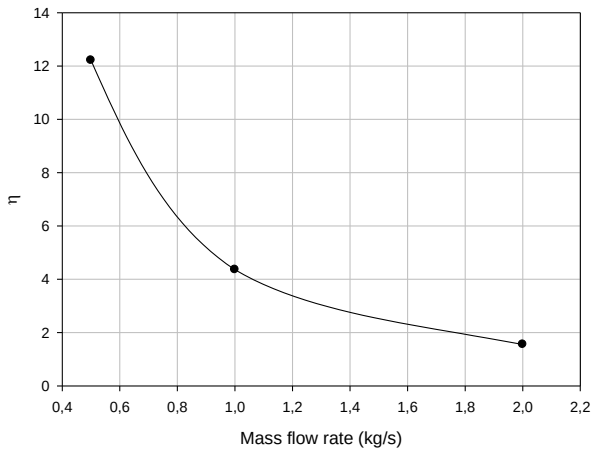

Figure 13. Overall performance factor

4.5 Performance of the heat exchanger

Table 4 shows the evolution of the temperature, the heat transfer coefficient, the pressure drop, the total heat transfer rate, the pumping costs calculated in the two heat exchangers studied. The heat transfer coefficient, the pressure drop, the total heat transfer rate, the pumping costs increase by 1.86% and 21.67% and 1.11%, and 21.68% successively. The baffle favors vortices over the simple flow case, and increasing the Reynolds number greatly increases the rate of heat transfer by introducing large recirculation zones.

Table 4. Performance of the heat exchanger without baffles and with baffles

Parameter	Without baffles	With baffles
T (°K)	322,51	325,15
h (W/m^{2}°K)	954,66	1779,55
ΔP (pa)	18,79	407,266
Q (W)	94182	105278
P (kW)	0,019	0,412

5. CONCLUSIONS

A numerical study based on the finite volume method using the SIMPLE algorithm is undertaken in this paper. It consists of stationary turbulent flow in forced convection mode, an incompressible fluid circulating inside a heat exchanger without and with baffles.

The profiles and the velocity fields as well as the profiles and the temperature distributions in the shell were obtained for all the geometry upstream, downstream of the baffles, the velocity profiles are more and more affected by the latter and the fluid is accelerating more and more as it moves towards the outlet of the shell.

The simple case assures us a high velocity along the shell, its measurement more than twelve times the reference velocity , the case with baffles ensures a velocity in the shell nineteen times higher than the reference velocity, the disturbance the higher and obtained upstream of the second baffle, the swirl zones are responsible for the increase in fluid temperature.

The pressure drop is a great importance in the design of the shell and tube heat exchangers because the pumping costs are strongly related to the pressure drop, and thus the decrease of the parameter results in lower operating costs.

The baffles direct the fluid and cause the appearance of a combined flow of two longitudinal and transverse spills, is the flow perpendicular to the tubes promotes heat transfer.

In the case of the presence of baffles, the flow along the shell is very complex because of the back-mixing, as a result these baffles significantly influence the pressure drop due to rapid changes in direction, expansion and contraction.

The exchanger performance in the case of presence of the baffles increases to 1.86% for the heat transfer coefficient, to 21.67% for the pressure drop, 2.46% for the Nusselt number, therefore, the baffles are expected to improve heat transfer and circulate the fluid in the shell according to an expected flow pattern.

REFERENCES

[1] Pan, M., Jamaliniy, S., Smith, R., Bulatov, I., Gough, M., Higley, T., Droegemueller, P. (2013). New insights to implement heat transfer intensification for shell and tube heat exchangers. Energy, 57: 208-221. https://doi.org/10.1016/j.energy.2013.01.017

[2] Master, B.I., Chunangad, K.S. Pushpanathan, V. (2003).

Fouling mitigation using helixchanger heat exchangers. Proceedings of the ECI Conference on Heat Exchanger Fouling and Cleaning: Fundamentals and Applications. https://dc.engconfintl.org/heatexchanger/43

[3] Saffarian, M.R., Fazelpour, F., Sham, M. (2019). Numerical study of shell and tube heat exchanger with different cross-section tubes and combined tubes. International Journal of Energy and Environmental Engineering, 10 (1): 33-46. https://doi.org/10.1007/s40095-019-0297-9

[4] Bhutta, M.M.A., Bashir, M.H., Khan, A.R., Ahmad, K.N., Khan, S. (2012). CFD applications in various heat exchangers design: A review. Applied Thermal Engineering, (32): 1-12. https://doi.org/10.1016/j.applthermaleng.2011.09.001

[5] Youcef-Ali, S. (2005). Study and optimization of the thermal performances of the offset rectangular plate fin absorber plates, with various glazing. Renewable Energy, 30(2): 271-280. https://doi.org/10.1016/j.renene.2004.04.009

[6] Youcef-Ali, S., Desmons, J.Y. (2006). Numerical and experimental study of a solar equipped with offset rectangular plate fin absorber plate. Renewable Energy, 31(13): 2063-2075. https://doi.org/10.1016/j.renene.2005.10.008

[7] Moummi, N., Youcef-Ali, S., Moummi, A., Desmons, J.Y. (2004). Energy analysis of a solar air collector with rows of fins. Renewable Energy, 29: 2053-2064. https://doi.org/10.1016/j.renene.2003.11.006

[8] Yang, Y.T., Hwang. C.Z (2003). Calculation of turbulent flow and heat transfer in a porous-baffled channel. International Journal of Heat and Mass Transfer, 46(5): 771-780. https://doi.org/10.1016/S0017-9310(02)00360-5

[9] Patankar, S.V., Sparrow, E.M. (1977). Fully developed flow and heat transfer in ducts having stream wise-periodic variations of cross-sectional area. Journal of Heat Transfer, 99: 180-186. https://doi.org/10.1115/1.3450666

[10] Kelkar, K.M., Patankar, S.V. (1987). Numerical prediction of flow and heat transfer in parallel plate channel with staggered fins. Journal of Heat Transfer, 109: 25-30. https://doi.org/10.1115/1.3248058

[11] Saim, R., Benzenine, H., Oztop, H.F., Al-Salem, K. (2013). Turbulent flow and heat transfer enhancement of forced convection over heated baffles in a channel effect of pitch of baffles. Journal of Numerical Methods for Heat & Fluid Flow, 23(4): 613-633. https://doi.org/10.1108/09615531311323773

[12] Lopez, J.R., Anand, N.K., Fletcher, L.S. (1996). Heat transfer in a three-dimensional channel with baffles. Numerical Heat Transfer, 30: 189-205. https://doi.org/10.1080/10407789608913835

[13] Yuan, Z.X., Tao, W.Q., Wang, Q.W. (1999). Numerical prediction for laminar forced convection heat transfer in parallel-plate channels with stream wise-periodic rod disturbances. International Journal for Numerical Methods in Fluids, 28: 1371-1387. https://doi.org/10.1002/(SICI)1097-0363(19981215)28:9<1371::AID-FLD774>3.0.CO;2-A

[14] Cheng, C.H., Huang, W.H. (1991). Numerical prediction for laminar forced convection in parallel-plate channels with transverse fin arrays. International Journal of Heat and Mass Transfer, 34(11): 2739-2749. https://doi.org/10.1016/0017-9310(91)90232-4

[15] Saim, R., Bouchenafa, R., Benzenine, H., Oztop, H.F., Al-Salem, K., Abboudi, S. (2013). A computational work on turbulent flow and heat transfer in a channel fitted with inclined baffles. Heat Mass Transfer, 49: 761-774. https://doi.org/10.1007/s00231-013-1121-3

[16] Guo, Z., Anand, N.K. (1997). Three-dimensional heat transfer in a channel with a baffle in the entrance region. Numerical Heat Transfer, Part A, 31(1): 21-30. https://doi.org/10.1080/10407789708914023

[17] Taher, F.N., Movassag, S.E., Razmi, K. (2012). Baffle space impact on the performance of helical baffle shell and tube heat exchangers. Applied Thermal Engineering, 44: 143-149. https://doi.org/10.1016/j.applthermaleng.2012.03.042

[18] Chang, B.H., Mills, A.F. (1993), Turbulent flow in a channel with transverse rib heat transfer augmentation. International Journal of Heat and Mass Transfer, 36: 1459-1469. https://doi.org/10.1016/S0017-9310(05)80056-0

[19] Yang, Y.T., Hwang, C.Z. (2003). Calculation of turbulent flow and heat transfer in a porous-based channel. International Journal of Heat and Mass Transfer, 46(5): 771-780. https://doi.org/10.1016/S0017-9310(02)00360-5

[20] Bazdidi-Tehrani, F., Naderi-Abadi, M. (2004). Numerical analysis of laminar heat transfer in entrance region of a horizontal channel with transverse fins. International Communications in Heat and Mass Transfer, 31(2): 211-220. https://doi.org/10.1016/S0735-1933(03)00226-4

[21] Li, H., Kottket, V. (1998). Effect of baffle spacing on pressure drop and local heat transfer in shell-and-tube heat exchangers for staggered tube arrangement. Journal of Heat Masse Transfer, 41(10): 1303-1311. https://doi.org/10.1016/S0017-9310(97)00201-9

[22] Dutta, P., Hossain, A. (2005) Internal cooling augmentation in rectangular channel using two inclined baffles. International Journal of Heat and Fluid Flow, 26: 223-232. https://doi.org/10.1016/j.ijheatfluidflow.2004.08.001

[23] Belmiloud, M.A., chemloul, N.S. (2015). Effect of baffle number on mixed convection within a ventilated cavity. Journal of Mechanical Science and Technology, 29: 4719-4727. https://doi.org/10.1007/s12206-015-1019-8

[24] Benzenine, H., Saim, R., Abboudi, S., Imine, O., Oztop, H.F., Abu-Hamdeh, N. (2018). Numerical study of a three-dimensional forced laminar flow in a channel equipped with a perforated baffle. Journal Numerical Heat Transfer, Part A: Applications, An International Journal of Computation and Methodology, 73(12): 881-894. https://doi.org/10.1080/10407782.2018.1486645

[25] Cucumo, M., Ferraro, V., Kaliakatsos, D., Mele, M., Galloro, A., Schimio, R., Le Pera, G. (2016). Thermohydraulic analysis of a shell-and-tube helical baffles heat exchanger. International Journal of Heat and Technology, 34(2): S255-S262. http://dx.doi.org/10.18280/ijht.34S210

[26] Dipankar De, Kanti Pal, T., Bandyopadhyay, B. (2017). Helical baffle design in shell and tube type heat exchanger with CFD analysis. International Journal of Heat and Technology, 35(2): 378-383. https://doi.org/10.18280/ijht.350221

[27] Ozden, E., Tari, I. (2010). Shell side CFD analysis of a

small shell-and-tube heat exchanger. Energy Conversion and Management, 51: 1004-1014. https://doi.org/10.1016/j.enconman.2009.12.003
[28] ANSYS Fluent Inc. (2006). Fluent 6.3 User's Manual. Fluent Inc. Centrera Resource Park, 10 Cavendish Court, Lebanon, USA.
[29] Patankar, S.V. (1980). Numerical heat transfer and fluid flow. Engineering & Technology, 214 pages. https://doi.org/10.1201/9781482234213

NOMENCLATURE

D_s	Shell size (mm)
d	Tube diameter (mm)specific
N_t	Number of tubes
L	Heat exchanger length (mm)
Nu	local Nusselt number along the heat source
T	Shell side inlet temperature (°K)
w	wall
B_c	Baffle cut (%)
N_b	Number of baffles
h	Heat transfer coefficient (W/(m^{2}K)
u, v, w	velocity components (m/s)
x, y, z	positions coordinates
$C_{1\varepsilon}$; $C_{2\varepsilon}$; C_μ	Constants of transport equations
m	Mass flow rate (kg/s)
f	Friction coefficient.
C_p	Specific heat at constant pressure, J/Kg.K
k	Turbulent kinetic energy
P	Pressure, Pa
Re	Reynolds number

Greek symbols

ε	dissipation rate of turbulence energy
ρ	Density, kg/m
ϕ μ_l, $\mu_t\mu_e$	Molecular, turbulent and effective viscosity, Pa.s
ν	Kinematics viscosity, pl
μ	dynamic viscosity, kg. m^{-1}.s^{-1}